Shear Thickening Fluids for Blast Wave Mitigation Applications: Preparation, Characterization and Numerical Modeling.

Abdallah Elsayed Gamal Elden
Military Technical College, Egypt, abdalla_gamal.el-den@outlook.com

Supervisors: Tamer Zakaria Wafy, Associate Professor. Hesham Ramzy Tantawy, Associate Professor.
Military Technical College, Egypt, tamer.z.wafy@hotmail.com, h.tantawy@staff.mtc.edu

Abstract– A shear thickening non-Newtonian fluid (STF) was prepared and studied for blast wave mitigation applications. STF was prepared by dispersing fumed silica (FS) particles within polyethylene glycol (PEG) by mechanical mixing. Average particle size of the dispersion was investigated by dynamic light scattering (DLS). A full rheological study was conducted with afterwards data processing to obtain governing equations for viscosity behavior over the thickening range using the non-Newtonian power law model. Blast threat was modulated using AUTODYN with further scaling to form better idea of equivalent threats. A numerical study was conducted using FLUENT concerning the blast loading attenuation capabilities of the prepared samples. Relatively high-loaded samples (10%, 15%) showed higher capabilities than other samples with the possibility of being incorporated in composite systems to enhance their mitigation abilities.

Keywords: Shear Thickening Fluids; Blast Load; AUTODYN; Fumed Silica; composite systems

I. INTRODUCTION

Throughout history, explosives have made their way among various materials and became well-established in many fields [1-4]. Explosives have proved to possess an extensively wide range of applications starting from the military field and using in war operations and ending with civil applications as blasting operations [2-5]. But as anything else, explosives grew to be a double-edged weapon. It became a major threat when related to terrorist attacks [6]. Almost any prosperous country has suffered from near or far from the impacts of a terrorist bombing attack. For this reason, the need for countermeasures grew even stronger than before.

Explosives countermeasures begin with prohibition of needed raw materials in the first place, passing by early detection and prevention [7, 8], ending with blast protection and effect mitigation as much as possible. Blast mitigation measures can either be active or passive [9]. Blast protection methods proves to be of great use whether the protected asset is an individual, a vehicle or even a building. Individuals benefiting from blast protection methods can be a VIP, a Peacekeeper, an IED team member or even an innocent person.

Despite the great need for blast mitigation research, this field of study still face a lot of challenges such as hardness of modeling of complex blast scenarios and understanding of the effect of charge geometry and detonation direction [9]. Hence, research in blast protection is essentially divided into two domains (a) understanding of propagation and loading from shock waves through different media, and (b) mitigation mechanisms [9]. These two fields incorporate multi-discipline study fields including chemistry, physics, fluid dynamics, computational mechanics and material science.

One blast mitigation means that interconnects fluid mechanics along with physics and material science is the use of non-Newtonian fluid especially dilatant fluids or mostly known as shear thickening fluids (STFs) [10-15]. Non-Newtonian fluids is another field of study that has its own methods, mechanisms and testing procedures[16-19]. A well-established method for modeling and predicting behavior of such fluid is the numerical method [19]. Numerical methods vary among using hydrocodes, computational fluid dynamics (CFD) or even artificial neural networks (ANN) [20]. Several models were put to represent the fluid behavior, these models include but are not limited to non-Newtonian Power law model[21], Cross model[22], Herschel-Buckley model [17, 18], Carreau model[21] and Casson model[16, 18].

Viscoelastic properties of fluid highly affect its governing model and properties[21, 23-25]. Fitting of STF behavior to the proposed models has repeatedly appeared in various literature concerning different disciplines [15, 19, 26]. However, a STF alone wouldn't be of great use in application without a reinforcer as high-performance fabrics or being integrated in a composite system to fully benefit from its properties [10-15].

II. EXPERIMENTAL

A. STF Preparation

Our Shear Thickening Fluid (STF) is a system of Fumed Silica (FS) dispersed in Polyethylene glycol (PEG). FS was Purchased from Cabot industries (CAS number: 112945-52-5, purity: 99+%, Density: 55 kg/m^3 and average particle size: 400 nm). PEG was Purchased from Oxford Lab. Chemicals with the following properties (CAS number: 25322-68-3, purity: 99+%, Density: 1125 kg/m^3 and average molecular weight: 400 g/mol). All utilized raw materials were used without any further modifications.

Mechanical Mixing at low shear rates below critical shear rates was utilized as a method of homogenization of the fluid. Mixing for prolonged time and addition of FS in small doses ensured the thorough distribution of silica within the dispersing medium to ensure high homogeneity of the sample and hence stable and homogeneous behavior[27].

Different loadings were prepared to estimate the sample loading effect as a factor. Table 1 shows the prepared samples numbers, abbreviations, corresponding loadings and apparent state.

TABLE 1
(PREPARED SAMPLES DATA)

Sample Number	Abbreviation	FS Loading (wt.%)	Apparent State
Sample 1	S1	1%	Viscous flowing liquid
Sample 2	S2	5%	Viscous flowing liquid
Sample 3	S3	10%	Heavy viscous liquid
Sample 4	S4	15%	Highly viscous liquid

This method was used along with addition of FS in small doses as beforementioned to avoid formation of Nano cluster agglomerations (NCAs) within the STF which may lead to differences in behavior throughout the same sample i.e. heterogenous distribution of FS.

B. Characterization of STF

All samples were inspected for average particle sizes using Malvern Instruments Zetasizer dynamic light scattering (DLS). A full rheological study was conducted for all samples using both oscillation and rotational modes of testing. Anton Paar Rheocompass rheometer was used to conduct this study. Data acquired were further analyzed for achieving maximum benefit.

C. Threat Identification

When concerning blast threats, there is a large variation reported in charge weights ranging from few kilograms to several hundred kilograms [6]. In here we considered an arbitrary threat consisting of 2kg TNT. The main destructive effect was considered to be the overpressure wave resulting from the charge explosion at 1m distance. Further scaling using Hopkinson-Cranz scaling law was conducted to form a better idea about equivalent charges at different distances.

Due to hardships faced, we couldn't obtain experimental data of the proposed charge explosion. So, we used hydrocodes as AUTODYN to obtain the pressure-time history of the proposed threat and used the obtained data in further numerical modeling of the fluid. Numerical modeling is well-established in various literature [13].

D. Numerical Model Construction

A numerical model was constructed using FLUENT Solver from ANSYS. Data from rheological measurements were fitted using power trend to obtain equations conforming to non-Newtonian power law. Fitted equations describing each sample behavior over its thickening range were obtained. These equations were used to describe the samples viscosity profiles in the numerical model.

Maximum overpressure value obtained from AUTODYN pressure-time history of the proposed threat was used as the main effect. Since pressure generated from explosion is dynamic pressure, it was converted to velocity in the fluid to ease its use within the model itself. This velocity value was set to the fluid interphase layer with the air transmitting the shockwave itself.

III. RESULTS AND DISCUSSION

A. Average Particle Sizes

From DLS readings obtained, it was found out that increasing FS loading in the sample increases the average particle size consequently. This happens as a result of particle-particle interaction which increases by increasing the sample loading. The dispersing medium forms hydrogen bonds with silica particles along its chain and forms a solvation layer around each hydrogen-bounded particle. Increasing the concentration decreases the thickness of the solvation layer covering each silica particle. This solvation layer prevents nearby particles from interacting with each other forming hydrogen bonds among each other.

Decreasing solvation layer thickness leads to higher chances of inter particles hydrogen bond formation. This formation of hydrogen bonds among particles causes the formation of clusters which in turn increases the average particle size of the dispersed particles. Table 2 shows the average particle size measured corresponding to each sample loading.

TABLE 2
(MEASURED AVERAGE PARTICLE SIZES)

Sample	Average Particle Size (nm)
S1	129.4
S2	255.2
S3	296.3
S4	305.4

B. Rheological Profiles

All samples showed the desired shear thickening behavior within a certain range. Each loading had a different critical shear rate at which thickening behavior commences but they were all near to 1 s^{-1}. Table 3 shows each sample's critical shear rate, initial viscosity, maximum viscosity and corresponding shear rate to maximum viscosity.

TABLE 3
(MEASURED RHEOLOGICAL VALUES)

Sample	Critical Shear Rate (s^{-1})	Initial Viscosity (Pa. s)	Maximum Viscosity (Pa. s)	Max. Vis. Shear Rate (s^{-1})
S1	1	0.0752	0.0798	2.51
S2	0.631	0.3585	1.0066	15.8
S3	1.58	4.7653	11.963	10
S4	1	43.365	67.347	2.51

The above results can give us an indication about the effect of sample loading on the rheological profile. Although increasing the loading increased the initial and maximum viscosities, it decreases the range in which the phenomena occurs as can be seen in S2, S3 and S4.

Here follows are the profiles of the samples. Each profile conforms to the previous given data and further confirms the conclusions.

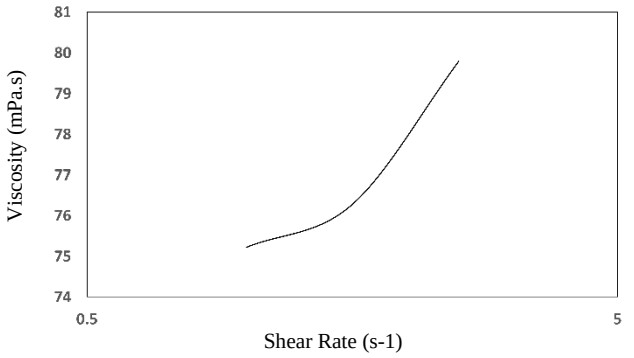

Figure 1 (S1 Rheological Profile)

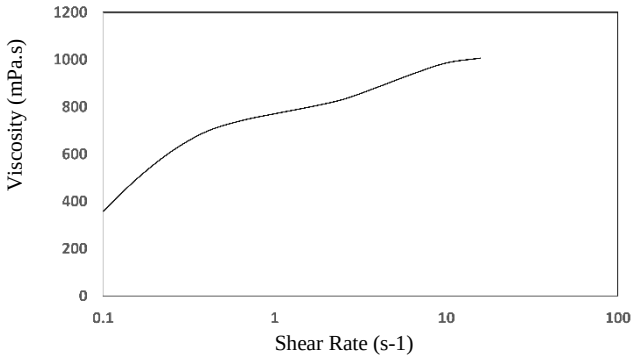

Figure 2 (S2 Rheological Profile)

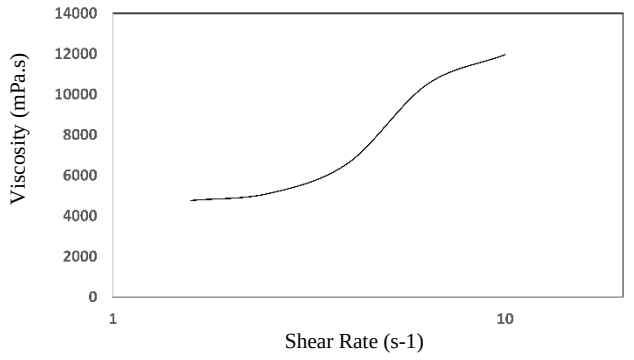

Figure 3 (S3 Rheological Profile)

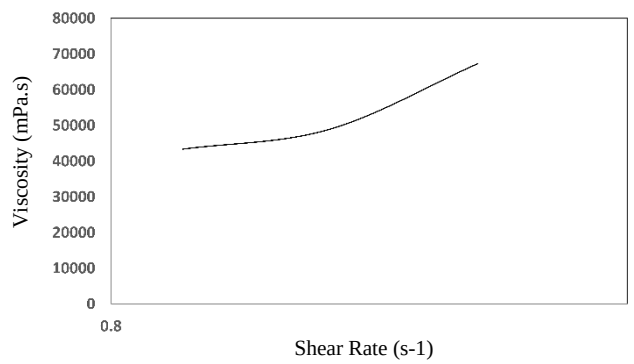

Figure 4 (S4 Rheological Profile)

These rheological profiles were curve fitted using power trend to conform with the non-Newtonian power law which states that ($\mu = k\dot{\gamma}^{n-1}$) where μ is the apparent viscosity, k is the consistency coefficient, $\dot{\gamma}$ is the shear rate and n is the power law index. Table 4 reports the curve fitted values representing each sample profile.

TABLE 4
(NON-NEWTONIAN POWER LAW COEFFICIENTS)

Sample	k	n
S1	0.0749	1.0641
S2	0.7046	1.1678
S3	3.38	1.5543
S4	41.959	1.4788

These values were used to modulate the fluid in the numerical model.

C. Viscoelastic behavior

All samples showed typical real fluid behavior where several behaviors were present in different regions of shear rate [28]. The samples showed shear thinning before entering the shear thickening region. Shear thickening region was followed by another shear thinning region which indicates that shear overtook the fluid structure.

Shear thickening and shear thinning behaviors can be interpreted using either hydro-clusters theory or order-disorder theory [16, 29]. A method to observe the viscoelastic state of the fluid at each shear rate was the phase shift angle (δ). Phase shift angle is determined for each sample from: $tan(\delta) = \frac{G''}{G'}$ where; δ is the phase shift angle, G" is the loss modulus and G' is the storage modulus [21, 23, 25]. G' represents the elastic solid behavior of the sample and G" represents the viscous solid behavior.

As the phase angle becomes more closer to zero, the sample behaves more dominantly as an elastic solid which is preferable [25]. Fig. (5) shows the phase shift angle of the samples at each shear rate with a point out to the lowest value. As it can be seen, increasing the loading shifts the lowest value position to higher shear rates which can be interpreted that higher loaded samples requires higher shear rates to behave more solid-like. S4 had the lowest phase shift angle as expected as it is the highest loaded sample.

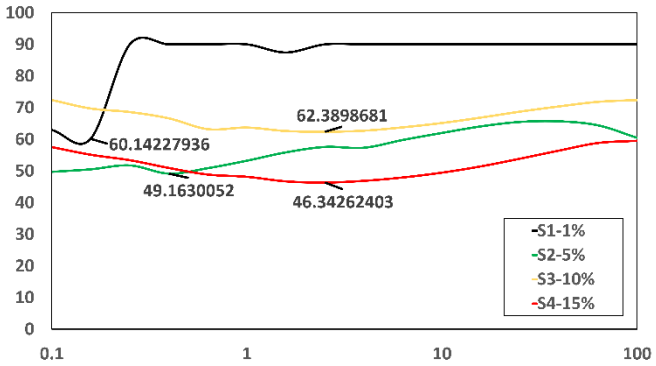

Phase Shift (Degree)

Angular Frequency (rad/s)

Figure 5 (Phase Shift Angles)

Throughout the thickening range, storage and loss modulus values were either close to each to other or storage modulus exceeded loss modulus value. This shows that our samples had the solid-like component more obvious in its behavior. Fig. (6) shows the storage and loss modulus trends of the samples throughout the whole inspected range of shear rates. Solid lines resemble storage modulus and dashed lines resemble loss modulus.

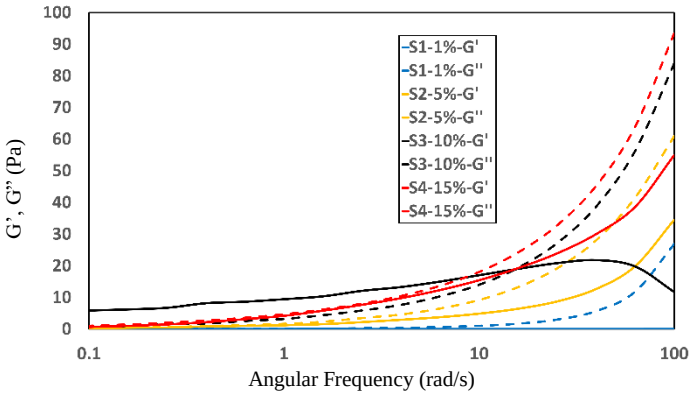

Figure 6 (G' & G" Trends)

D. *Threat Analysis*

The proposed threat of 2kg TNT charge at 1m distance from center of explosion was investigated using AUTODYN hydrocode from ANSYS. Fig. (7) shows the obtained pressure-time history from the prepared model with a point out to the maximum peak overpressure obtained. The model was set to idealized conditions as to obtain the maximum pressure that can be generated from such charge at the determined distance.

Using Hopkinson-Cranz scaling law [30], threat scaling was carried out to form an idea about equivalent charges which would give the same effect at arbitrary distances of 5, 10, 25, 50 and 100 meters. Hopkinson-Cranz law states that ($Z = \frac{R}{W^{1/3}}$), where: Z is the scaling distance, R is the distance from charge center and W is the charge weight. Table 5 shows the equivalent charge weights at the proposed arbitrary distances.

TABLE 5
(EQUIVALENT CHARGE WEIGHTS AT ARBITRARY DISTANCES)

Distance (m)	Equivalent Charge (kg TNT)
5	250
10	2000
25	31250
50	250000

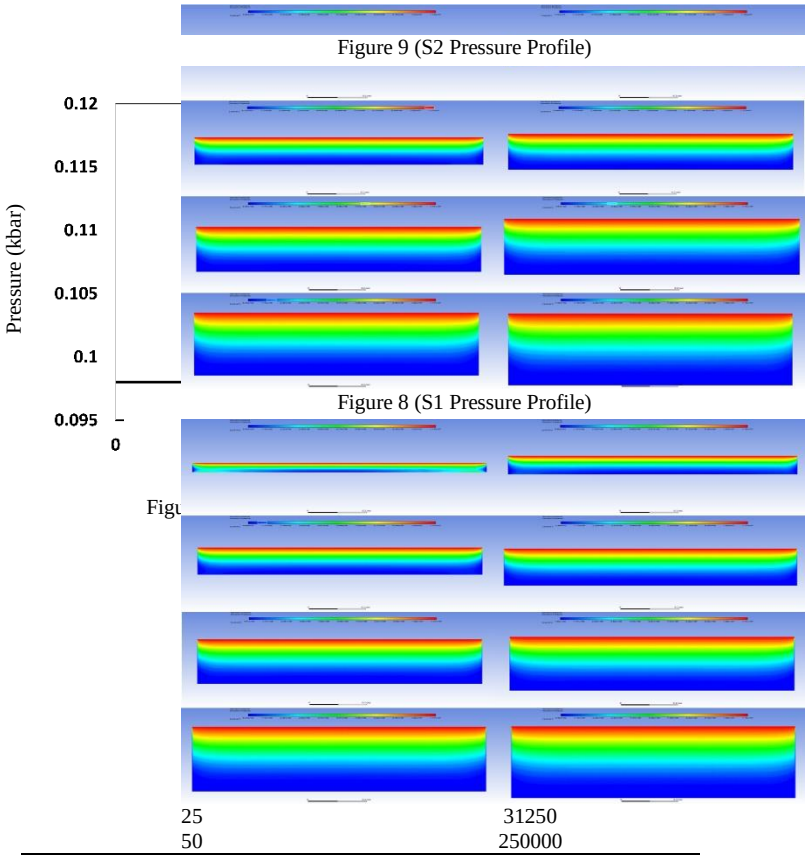

Figure 9 (S2 Pressure Profile)

Figure 8 (S1 Pressure Profile)

Figu

E. *Numerical Model Results*

The model was constructed using FLUENT hydrocode from ANSYS. The main effect used was the maximum peak overpressure value obtained from AUTODYN. Using Bernoulli's equation, this value of dynamic overpressure was converted to velocity of the fluid layer in contact with air transferring the shockwave originally [18].

The test specimen was designed in shape of a rectangular slab of fluid having a width of 1m and varying thickness. Several thicknesses were investigated to form an idea about the variation of pressure and velocity profiles within the fluid with changing thickness. We used thicknesses from 5 to 40cm with a 5cm step.

All samples were able to attenuate the acting pressure to some point. Samples with lower loadings were able to attenuate the acting pressure to below dangerous values at high thicknesses, while higher loaded samples were able to carry out the same action at lower thicknesses. But generally, all samples were able to drop the incident pressure to below the fatal pressure value which is 1.8 bar. Figures from

(8-11) shows S1, S2, S3 and S4 pressure profiles respectively at the tested thicknesses.

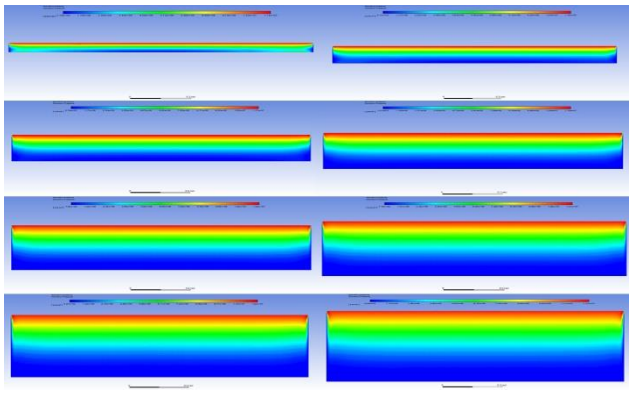

Figure 10 (S3 Pressure Profile)

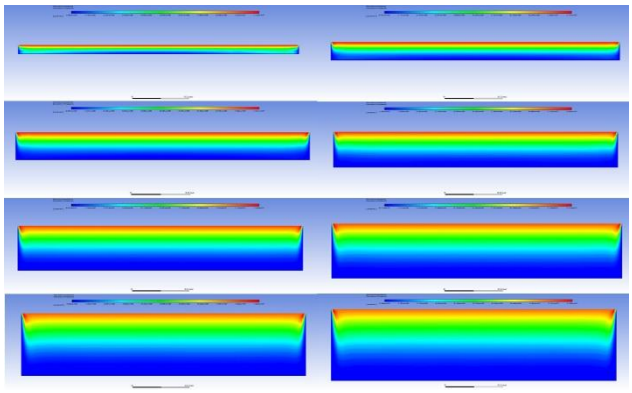

Figure 11 (S4 Pressure Profile)

As beforementioned, all the samples were able to attenuate the incident pressure below the fatal value of 1.8 bar. Table (6) shows the ratio of the minimum pressure value in these profiles to the atmospheric pressure.

TABLE 6
(RATIO OF ATTENUATED PRESSURE TO ATMOSPHERIC PRESSURE)

Thickness (cm)	Sample			
	S1	S2	S3	S4
5	1.393	1.338	1.21	1.188
10	1.121	1.098	1.06	1.054
15	1.06	1.044	1.028	1.025
20	1.034	1.024	1.016	1.014
25	1.023	1.015	1.01	1.01
30	1.016	1.011	1.007	1.007
35	1.007	1.005	1.005	1.005
40	1.007	1.005	1.004	1.004

Figures from (12-15) shows the values of maximum incident pressure and minimum attenuated pressure for S1 to S4 respectively.

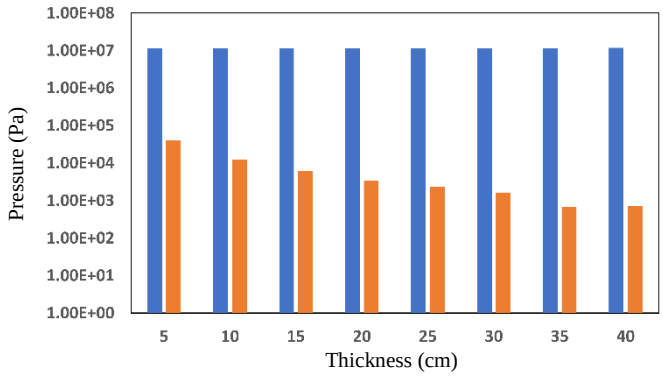

Figure 12 (S1 Affecting and Attenuated Pressure)

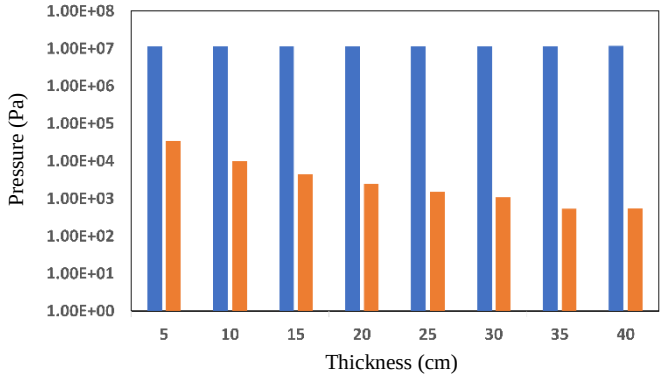

Figure 13 (S2 Affecting and Attenuated Pressure)

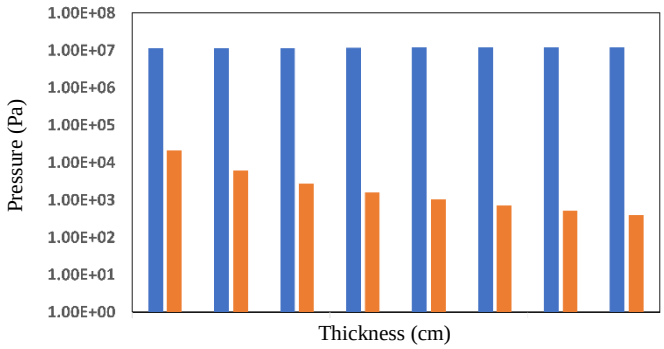

Figure 14 (S3 Affecting and Attenuated Pressure)

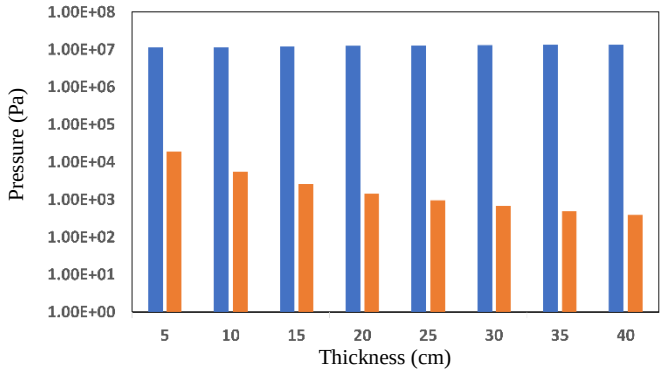

Figure 15 (S4 Affecting and Attenuated Pressure)

These values of affecting and attenuated pressures were fitted to a power function ($y = mx^n$) which can be used to predict the attenuated pressure at any arbitrary thickness within the tested range. Coefficients of the fitted equations along with r-squared values are given in Table 7.

TABLE 7
(COEFFICIENTS OF FITTED PRESSURE EQUATIONS)

Sample	m	n	R^2
S1	46737	-1.974	0.9794
S2	38729	-2.052	0.9909
S3	22222	-1.916	0.9996
S4	19734	-1.882	0.9997

Boundary conditions within the model was carefully set as to avoid end effects of the walls as they were set as no slip walls. Velocity profiles show this effect as the velocity of the boundary layer stick to the walls will equal zero.

Velocity profiles can also be used to determine the exit velocity of the wave to the surrounding air and then reconvert it to pressure to find out the exact amount of pressure passing through the fluid. Figures from (16-19) show the velocity profiles for S1 to S4 respectively.

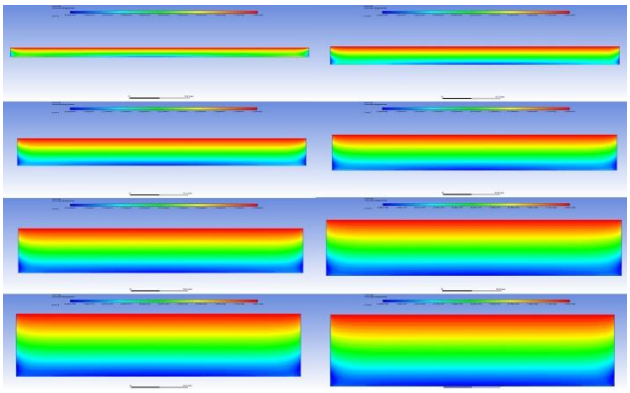

Figure 16 (S1 Velocity Profile)

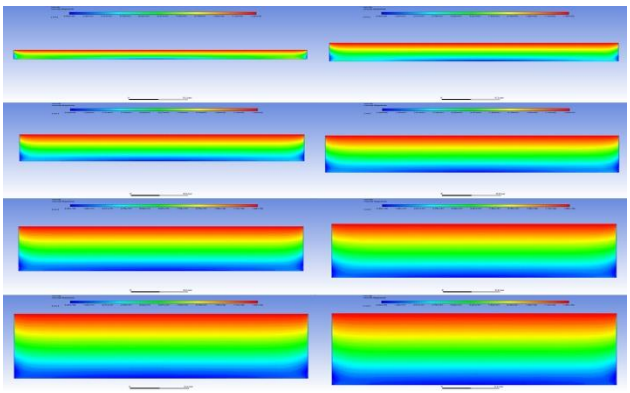

Figure 17 (S2 Velocity Profile)

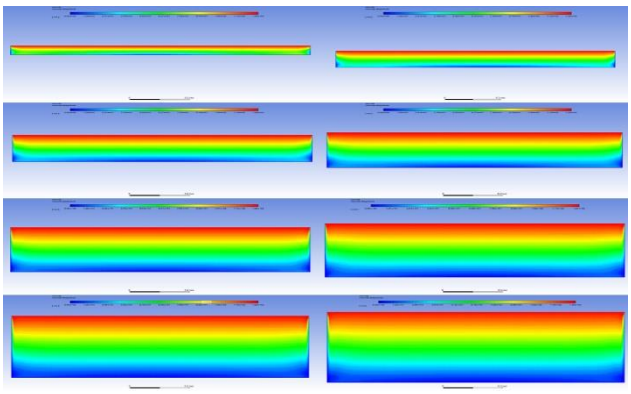

Figure 18 (S3 Velocity Profile)

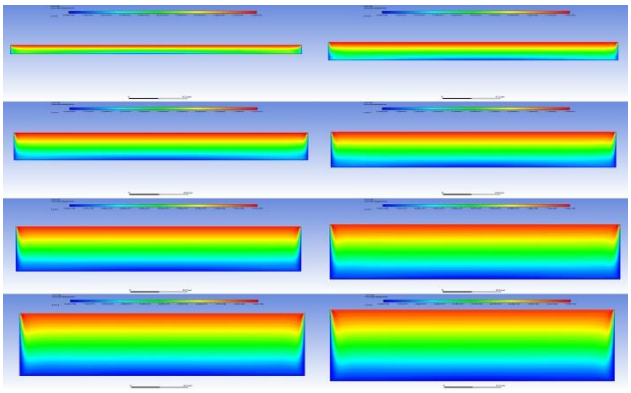

Figure 19 (S4 Velocity Profile)

IV. CONCLUSION

STF samples were prepared and characterized by DLS and full rheological study. Average particle size within the suspension was found to increase by increasing FS loading. Prepared samples were found to conform with non-Newtonian power law within their thickening region. Governing equations for viscosity behavior within this region was obtained and utilized in construction of a numerical model using FLUENT hydrocode. Proposed threat data was obtained using AUTODYN hydrocode due to hardships faced that prevented us from obtaining experimental data. All samples showed the desired mitigation ability to varying extents. Samples with higher loadings showed the most promising behavior and showed readiness to be incorporated in a composite system for further performance enhancement.

ACKNOWLEDGMENT

Thanks is due to the ones who deserve, and it is due to my supervisors who have supported and guided me through the whole research process. Special Thanks is also due to Chemical Engineering Branch within the Military Technical College. Finally, the whole credit goes back to my family for the support, love and care they showed through years I spent studying. For all mentioned, thank you.

REFERENCES

1. Urbanski, T., S. Laverton, and W. Ornaf, *Chemistry and technology of explosives*. Vol. 1. 1964: pergamon press New York, NY.
2. Roy, P.P., *Rock blasting: effects and operations*. 2005: CRC Press.
3. Hay, D.R., *Explosive Welding: Applications and Techniques*, in *High-Pressure Science and Technology: Volume 1: Physical Properties and Material Synthesis / Volume 2: Applications and Mechanical Properties*, K.D. Timmerhaus and M.S. Barber, Editors. 1979, Springer US: Boston, MA. p. 1813-1836.
4. Mahadevan, E.G., *Ammonium nitrate explosives for civil applications: slurries, emulsions and ammonium nitrate fuel oils*. 2013: John Wiley & Sons.
5. Jitea, I.-C., et al., *Verification of Performance Requirements and Technical Parameters of Plastic Explosives with Civil and Military Use.* 2019. **19**(1.3): p. 725-732.
6. Pizam, A. and G. Smith, *Tourism and Terrorism: A Quantitative Analysis of Major Terrorist Acts and Their Impact on Tourism Destinations.* Tourism Economics, 2000. **6**(2): p. 123-138.
7. Moore, D.S.J.S. and I.A.I. Journal, *Recent advances in trace explosives detection instrumentation.* 2007. **8**(1): p. 9-38.
8. Steinfeld, J.I. and J.J.A.r.o.p.c. Wormhoudt, *Explosives detection: a challenge for physical chemistry.* 1998. **49**(1): p. 203-232.
9. Mostert, F.J., *Challenges in blast protection research.* Defence Technology, 2018. **14**(5): p. 426-432.
10. Decker, M., et al., *Stab resistance of shear thickening fluid (STF)-treated fabrics.* 2007. **67**(3-4): p. 565-578.
11. Egres Jr, R., et al., *Stab resistance of shear thickening fluid (STF)–Kevlar composites for body armor applications*, in *Transformational Science And Technology For The Current And Future Force: (With CD-ROM)*. 2006, World Scientific. p. 264-271.
12. Fu, K., et al., *Low-velocity impact behaviour of a shear thickening fluid (STF) and STF-filled sandwich composite panels.* Composites Science and Technology, 2018. **165**: p. 74-83.
13. Park, Y., et al., *Numerical simulation and empirical comparison of the high velocity impact of STF impregnated Kevlar fabric using friction effects.* 2015. **125**: p. 520-529.
14. Wetzel, E.D., et al., *The Effect of Rheological Parameters on the Ballistic Properties of Shear Thickening Fluid (STF)-Kevlar Composites.* AIP Conference Proceedings, 2004. **712**(1): p. 288-293.
15. Zhang, X.Z., W.H. Li, and X.L. Gong, *The rheology of shear thickening fluid (STF) and the dynamic performance of an STF-filled damper.* Smart Materials and Structures, 2008. **17**(3): p. 035027.
16. Chhabra, R.P., *Non-Newtonian Fluids: An Introduction*. 2010, Springer New York. p. 3-34.
17. Anderson, J.D. and J. Wendt, *Computational fluid dynamics*. Vol. 206. 1995: Springer.
18. Batchelor, C.K. and G. Batchelor, *An introduction to fluid dynamics*. 2000: Cambridge university press.
19. Crochet, M.J. and K. Walters, *Numerical Methods in Non-Newtonian Fluid Mechanics.* Annual Review of Fluid Mechanics, 1983. **15**(1): p. 241-260.
20. Gürgen, S., M.A. Sofuoğlu, and M.C. Kuşhan, *Rheological modeling of multi-phase shear thickening fluid using an intelligent methodology.* Journal of the Brazilian Society of Mechanical Sciences and Engineering, 2020. **42**(11).
21. Phan-Thien, N , Author and Rossikhin, YA , Reviewer, *Understanding Viscoelasticity: Basics of Rheology.* Applied Mechanics Reviews, 2004. **57**(1): p. B4-B4.
22. MM, C., *Rheology of non-Newtonian fluids: a new flow equation for pseudoplastic systems.* Journal of Colloid Science, 1965. **20**: p. 417-437.
23. Christensen, R., *Theory of viscoelasticity: an introduction*. 2012: Elsevier.
24. Franck, A. and T.J.T.I. Germany, New Castle, DE, USA AN004, *Viscoelasticity and dynamic mechanical testing.* 1993.
25. Roylance, D., *Engineering viscoelasticity.* Department of Materials Science and Engineering–Massachusetts Institute of Technology, Cambridge MA, 2001. **2139**: p. 1-37.
26. Katarina, S., *The role of different rheological models in accuracy of pressure loss prediction.* Rudarsko-Geološko-Naftni Zbornik, 2004. **16**.
27. Hemmat Esfe, M. and H. Rostamian, *Non-Newtonian power-law behavior of TiO2/SAE 50 nano-lubricant: An experimental report and new correlation.* Journal of Molecular Liquids, 2017. **232**: p. 219-225.
28. Picard, D. and P.J.T.C.J.o.C.E. Bishnoi, *The importance of real-fluid behavior and nonisentropic effects in modeling decompression characteristics of pipeline fluids for application in ductile fracture propagation analysis.* 1988. **66**(1): p. 3-12.
29. Wang, S.Q.J.M., *Transient network theory for shear-thickening fluids and physically crosslinked networks.* 1992. **25**(25): p. 7003-7010.
30. Masi, F., I. Stefanou, and V.J.a.p.a. Maffi-Berthier, *Scaling laws for the rigid-body response of masonry structures under blast loads.* 2020.